Accepted Manuscript

2,4-dihydroxy benzaldehyde derived Schiff bases as small molecule Hsp90 inhibitors: Rational identification of a new anticancer lead

Sayan. Dutta Gupta, B. Revathi, Gisela.I. Mazaira, Mario.D. Galigniana, C.V.S. Subrahmanyam, N.L. Gowrishankar, N.M. Raghavendra

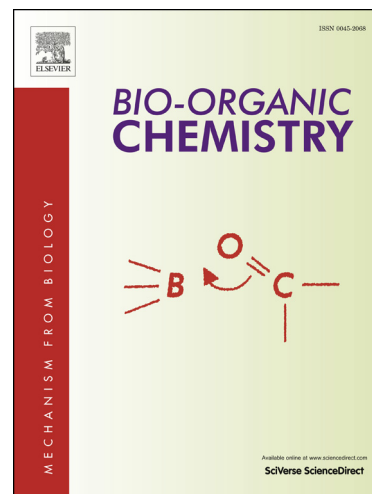Please cite this article as: Sayan. Dutta Gupta, B. Revathi, Gisela.I. Mazaira, Mario.D. Galigniana, C.V.S. Subrahmanyam, N.L. Gowrishankar, N.M. Raghavendra, 2,4-dihydroxy benzaldehyde derived Schiff bases as small molecule Hsp90 inhibitors: Rational identification of a new anticancer lead, *Bioorganic Chemistry* (2015), doi: http://dx.doi.org/10.1016/j.bioorg.2015.02.003

2,4-dihydroxy benzaldehyde derived Schiff bases as small molecule Hsp90 inhibitors: Rational identification of a new anticancer lead

Sayan Dutta Gupta[a,b], B. Revathi[a], Gisela.I.Mazaira[d], Mario.D.Galigniana[d,e], C.V.S. Subrahmanyam[a], N.L. Gowrishankar[c] and N.M. Raghavendra[a]

[a]*Department of Pharmaceutical Chemistry, Gokaraju Rangaraju College of Pharmacy, Osmania University, Hyderabad, India.*
[b]*R&D centre, Department of Pharmaceutical Sciences, Jawaharlal Nehru Technological University, Hyderabad, India.*
[c]*Swami Vivekananda Institute of Pharmaceutical Sciences, Nalgonda, Andhrapradesh, India*
[d] *Department of Biological Chemistry, Faculty of Natural Sciences, University of Buenos Aires, Argentina*
[e]*Institute of Experimental Biology and Medicine-CONICET, Argentina.*

* Corresponding author. E- mail: sayanduttagupta1@rediffmail.com

Ph: +91-40-3291 2927, Fax: +91-40-2304 0860;

1. INTRODUCTION

Heat shock protein (Hsp90) is an ATP dependant molecular chaperone required for the repair of several signaling proteins which promote cancer cell multiplication and survival [1, 2]. Hence, the pharmacological inhibition of this chaperone leads to simultaneous blockage of multiple oncogenic transduction signal pathways, thus making it an attractive anticancer target [3, 4]. The energy required for its chaperoning function is acquired from the hydrolysis of ATP which binds to the N-terminal domain of the protein [5, 6]. This ATP binding cleft is structurally different from most ATP-utilizing vital enzymes of normal cells [7-9]. Moreover, Hsp90 is overexpressed in cancer cells in association with co-chaperones whereas Hsp90 of normal tissues resides in a free and uncomplexed state [10, 11]. The above observations were supported by studies employing various Hsp90 inhibitors wherein it was proved that cancer cells are more sensitive to Hsp90 inhibition compared to healthy cells [12, 13]. These conclusions further affirm the notion that suppression of Hsp90 function can lead to selective killing of cancer cells over normal cells. All the aforementioned research findings gave the impetus to develop novel small molecule chemotypes against Hsp90 with reduced toxic side effects.

Molecular docking is a fast and efficient computational technique that helps a drug design process to dramatically widen the chemical space and reduce the number of molecules for experimental verification [14]. Considering the pivotal role resorcinol moiety plays in Hsp90 suppression [15, 16] and the importance of schiff bases (imines or azomethines) in cancer chemotherapy [17, 18], we began our Hsp90 research program with structure based drug design of novel resorcinol containing imines using Malachite green assay which measures the ATPase activity of human Hsp90 [19]. This effort led to the discovery of a series of novel small molecule azomethines as Hsp90 inhibitors. Compound **A** and **B** with an IC_{50} value of 3nm and 4nm respectively were found to be the most potent ones (**Fig. 1**). Unfortunately, these two compounds exhibited an IC_{50} value greater than 15μM in the cell viability assay against PC3 prostate cancer cell lines performed by adopting 3-(4,5-dimethythiazol- 2-yl)-2,5-diphenyl tetrazolium bromide (MTT) assay methodology [19]. The large difference between biochemical and cellular potencies of the compounds may be attributed to the presence of any reactive and/or unstable functional groups. However this hypothesis can be ascertained by comparing the activity profile of larger number of resorcinol scaffold bearing imines. Furthermore, the structure of the most promising imine (**Fig. 2**) of our study did not offer any scope for further chemical modifications. Hence the research effort was not able to generate any lead molecule for subsequent optimization. Moreover not a single compound inhibited 50 percent of cancer cells below 5μM concentration and thus making them poor candidates for further pre-clinical evaluation in animals. All the above mentioned limitations of the earlier research work prompted us to rationally design few more 2,4-dihydroxybenzaldehyde derived Schiff bases (**Fig. 3**) with our established docking protocol[20]. The ligands predicted to possess better protein affinity were synthesized and characterized by IR, NMR and mass spectral analysis. These imines were evaluated for their Hsp90 inhibition potential by utilizing the colorimetric malachite green assay. The azomethines were further screened for their antiproliferative effect against PC3 carcinoma cell lines by using the MTT assay protocol. Therefore the main objective of this study is to rationally identify Hsp90 selective low molecular weight antineoplastic chemical lead among 2,4-dihydroxy benzaldehyde derived imines. This will guide medicinal chemist worldwide to discover more efficacious drug molecules against cancer with fewer toxic side effects. Subsequently the proposed compounds would add further structural diversity to the field of dihydroxy phenyl

imines as Hsp90 inhibitors with an additional insight into the functional groups that can be accommodated in the Hsp90 N-terminal ATP-binding cleft for this class of compounds.

2. Materials and Methods

2.1. Molecular Modeling methods

Molecular modeling was carried out by docking ligands into the protein active site with Surflex Geom X tool of Sybyl X-1.2 version software installed on a Windows based Dell Precision T-1500 workstation. PDB entry 3EKR (a co-crystal structure of 4-{[(2R)-2-(2-methylphenyl)pyrrolidin-1-yl]carbonyl}benzene- 1,3-diol in complex with human Hsp90 with a resolution of 2Å)[21] was used for executing the docking studies. Four binding site waters (902, 903, 981 and 1026) were retained in the docking process as they provide key interactions required for stabilizing the ligand in the active site [20, 22-24]. This was followed by addition of hydrogens for the receptor and waters. Subsequently, the protein was energy minimized using AMBER7 FF99 force field and the protomol was generated by maintaining 0.5 Å threshold factor and 0 Å bloat. [25-27]. The structures of the compounds were built using Chem draw ultra 8.0 and exported as mol files to Schrodinger software (Maestro, 9.1 versions) where they were converted into SD file format for Sybyl compatibility. Finally a clean, energy minimized, 3D conformation of the ligands were generated and subsequently docked at the developed protomol of the prepared protein [28, 29].

2.2. Synthesis of Compounds

The chemical reagents and solvents were commercially available from Hi-media Laboratories Private Limited and were used without further purification. The termination of the reaction was confirmed by performing thin layer chromatography on aluminium sheets coated with silica gel G containing fluorescent indicators, F_{254}. The mobile phase for the development of the plate was ethyl acetate and petroleum ether (1:1). Melting point values were determined on a DRK Digital melting point apparatus and are reported uncorrected. IR spectra were recorded using KBr powder on Shimadzu diffuse reflectance attachment (DRS-800) mounted on a Shimadzu IR-Affinity spectrometer. ^{1}H NMR spectra were obtained on a Bruker Avance 300 MHz instrument in DMSO-d_6 (Tetramethylsilane as the internal standard). Chemical shift values are reported in parts per million (δ, ppm). Mass spectra were run using a atmospheric pressure-electron spray ionization 6120 Quadrupole LC/MS mass spectrometer (Agilent Technologies, California, USA).

2.2.1. Synthesis of 2,4-Dihydroxy benzaldehyde [19, 30]

This was synthesized according to a previously described procedure (**Fig. 4**). Phosphorous oxychloride(0.026 mol) was added dropwise to a solution of dimethyl formamide (0.030 mol) in acetonitrile (7ml) at 22°C to 28°C and stirred for 1 h at the above temperature. This was followed by addition of resorcinol (0.022 mol) in acetonitrile (7ml) at -15 to -17°C. The reaction mixture was then stirred for 2 h at this temperature and then at 28-32°C for 1h. The mixture was cooled to 5°C and after stirring for 1h the Vilsmeier formamidinium phosporodichloride salt gets precipitated which was filtered and washed with cold acetonitrile. This intermediary salt was added in two parts to a beaker containing 60 ml of water at 40°C. The solution was then heated

to 52°C for 30 min after which it was left to cool at 35°C. Subsequently, 1ml of 0.09M sodium thiosulfate solution was added until the pink color disappears. The reaction was cooled to 5°C and stirred for 2 h to precipitate a white solid. The white solid was filtered, washed with cold water and air dried for 2 h to obtain white crystals of 2,4-dihydroxy benzaldehyde.

2.2.2. General procedure for the synthesis of Schiff base derived from 2,4-Dihydroxy benzaldehyde [19]

Synthesis of the imines was achieved according to a method outlined in the scheme (**Fig. 4**). The appropriate amine (5 mmol) was heated at reflux with 2,4-dihydroxy benzaldehyde (5 mmol) in absolute ethanol for 3 h. The completion of the reaction was confirmed by TLC. It was followed by addition of water that resulted in the formation of colored precipitate which was filtered and air dried. The resulting solid was recrystallized from aqueous ethanol to obtain the pure product.

2.2.3. Synthesis of 2-(4-aminophenyl) benzimidazole (amine used in the preparation of schiff base 13) [31]

o-phenylenediamine (0.00924 moles) and *p*-amino benzoic acid (0.00924 moles) was transferred to a round bottom flask containing 6.5 ml of polyphosphoric acid. The reaction mixture was refluxed at 100°C for 3 h. It was cooled and neutralized with 10% sodium carbonate solution. The precipitate formed was filtered and washed with cold water. The solid obtained was dried and recrystallized from methanol/water to obtain the pure product.

The general structure of the ligands along with the numbering system used in this work is shown in **Fig. 3.**

2.3 Malachite green assay for Hsp90 ATPase suppression

Histidine-tagged human Hsp90 (hHsp90β) was kindly provided by Dr. Chrisostomos Prodromou, University of Sussex, United Kingdom. The chaperone was further purified and expressed according to a previously described procedure[6, 32]. The ATPase assay procedure was performed by incubating 10µg of pure hHsp90β along with the compounds (diluted in DMSO) for 10 min at 20°C in a buffer containing 50 mM Hepes at pH 7.5, 6 mM $MgCl_2$, 20 mM KCl, and 1 mM ATP[32-34]. To stop the incubation, two volumes of malachite green reagent were added to each well of the plate. The plate was shaken and left to stand at room temperature for about 25 minutes, and the absorbance at 630 nm was measured[35, 36]. Geldanamycin was taken as the standard reference compound.

2.4. *In vitro* cell growth assay

PC3 prostate cancer cells were utilized for the study. Cellular growth in the presence or absence of experimental agents was determined using the previously reported MTT[3-(4, 5-dimethylthiazol-2-yl)-2,5-diphenyl tetrazolium bromide] assay[37, 38]. The cell lines was cultured in RPMI1640 (Invitrogen)/10% fetal bovine serum (Gibco) medium supplemented with 0.007% streptomycin and 0.002% penicillin. The cells were then counted and incubated for 37°C with 5 % CO_2 in a 96 well micro plates. When the cells reach 80% confluence, they were treated with the test compounds and standard (geldanamycin) prepared in DMSO to furnish the

4

concentration range of study, 0.1µM-5µM. Control wells contained equivalent volume of the vehicle. This was followed by 48 h incubation after which 5µl of MTT reagent along with 45 ml of phenol red and FBS free DMEM was added to each well. Thereafter the plates were incubated at 37 °C with 5 % CO_2 for 4 h. Subsequently, 50 ml of solubilization buffer was added to each well to solubilize the colored formazan crystals produced by the reduction of MTT. After 48 hrs, the optical density was measured at 550nm using spectrophotometer in a microplate reader (Bio-Rad, USA)[39].

3. Results and Discussion

3.1. Molecular Design

The docking protocol was validated by comparing the software generated ligand-Hsp90 binding interactions with the crystallographic analysis available from PDB and its corresponding literature. It was reported that 2'-hydroxyl group of the native ligand interacted with Asp 93 and water molecule 902 via hydrogen bond. The 4'- hydroxyl group formed hydrogen bond interaction with amino acid Asn 51 and water molecule 903. The other prominent hydrogen bond contacts detected was between the carbonyl oxygen and amino acid Thr 184. Further analysis indicated that the pyrrole moiety occupied a hydrophobic area formed by Met 98, Ile 96, Ala 55 and Lys 58. The other significant hydrophobic affinity was observed between phenyl ring and amino acid Tyr, Val 136 and Gly 135. The amino acid residue of Leu 107, Val 150 and Gly 135 formed a hydrophopic region where the resorcinol moiety was embedded. These interactions were found matching with the reported crystallographic data (**Fig. 5a** and **5b**).

The Surflex Geom X docking program predicted thirteen compounds as effective Hsp90 inhibitor. The detailed result of ligand-Hsp90 binding studies is shown in **Table 1.** These molecules were found to form hydrogen bond contact with Asp54, Asp93, Asn51, Asn106, Gly 97, Lys58, Thr184 and water molecule 902, 903 981 and 1026. The H- bond contact of 4'-OH and 2'-OH with Asp93/water 902 and Asn51/water 903 respectively was revealed for majority of the compounds. The highest scored compound (**3**) disclosed additional hydrogen bond contact with amino acid residue Asn 106, Lys 58 via oxygen of para nitro group. A hydrogen bond between water number 1026 and ortho nitro group was also observed for compound **3 (Fig. 6a).** The hydrophobic interactions of the Schiff bases revealed that the dihydroxy phenyl moiety along with the imine part is embedded in a hydrophopic pocket of Val 186, Ile 91, Phe 138, Val 150 and Leu 48. The phenyl ring attached to the imine nitrogen was found to occupy a pocket surrounded by amino acid Ala 55, Met 98 and Leu 107 (**Fig. 6b**).

3.2. Synthesis

The series of imines derived from 2,4-dihydroxy benzaldehyde were characterized by melting point, Rf values, IR, ^{1}HNMR and mass spectroscopy. All the relevant data regarding characterization of compounds is presented in **Table 2.**

The FT-IR spectra of the synthesized compounds showed absorption bands at 1645-1614 cm^{-1} for imines. The broadness of the OH band observed between 3751-3311 cm^{-1} may be attributed to the intramolecular hydrogen bond between CH=N (imine nitrogen) and OH (phenolic) group [40, 41]. The phenolic C-OH stretching vibrations were confirmed by medium intensity bands in the range of 1284-1049 cm^{-1}. The presence of additional bands between 1598 and 1419 cm^{-1}

were characteristic of C=C bands of the aromatic rings. Compound **3** displayed two bands at 1510 and 1130 corresponding to N-O stretching. A stretching vibration band at 1122 cm-[1] for compound **8** was attributed to its C–F bond.

In the ^{1}HNMR spectroscopy, the absence of CHO proton signal at 9.92 and the appearance of sharp imine singlet at 9.24-8.03 confirmed the formation of schiff bases. The signal corresponding to the 2'- hydroxyl groups was shifted downfield because of intramolecular hydrogen bonding between it and the nitrogen of imine (OH----N=C) [42, 43].

The mass spectra of the compounds displayed base peak at M^+ and M^++1 corresponding to their respective molecular weight.

3.2.1. Vilsmeier formamidinium phosphoro dichloridate sal [19]

IR (KBr cm^{-1}): 3022-2650(OH, CH, P-OH stretching); 1643(C=N stretching); 1614, 1583, 1517, 1346(P=O stretching, free/bonded and C-O stretching); 1109, 1076 (P-O-C stretching); 555, 528, 493(P-Cl vibration).

3.2.2. 2,4-Dihydroxy benzaldehyde[19]

IR (KBr cm^{-1}): 3103 (OH-stretching); 3037 (C-H aromatic stretching); 2848 (C-H stretching aldehyde); 1628(C=O stretching, aldehyde); 1496 (C=C aromatic stretching); 1395 (C-H bending aldehyde); 1228 (C–OH stretching). ^{1}HNMR (DMSO, 400 MHz) δ: 10.84 (s, 1H, OH); 10.83 (s, 1H, OH); 9.92 (s, 1H, O=CH); 7.51 (d, 1H, Ar-H, J = 8.8 Hz); 6.40 (dd, 1H, Ar-H, ABX; J_{BA} = 8.8 Hz, J_{BX} = 2.0 Hz); 6.31(d, 1H, Ar-H, J_{BX} = 2.0 Hz). Mass (m/z): 137 (M-1)$^-$ (base peak).

3.3.3. 2-(4-aminophenyl) benzimidazole [31]

IR (KBr cm^{-1}): 3400, 3360 (primary N-H stretching), 3048 (aromatic C-H stretching), 1500, 1446 (C=C aromatic stretching); 1400, 1375 (thiazole skeletal bands).

3.3.4. 4-(hydrazonomethyl)benzene-1,3-diol (1)

IR (KBr cm^{-1}): 3518, 3469 (NH str); 3217(OH-str); 2995 (Ar, C-H str); 1616 (C=N str); 1521, 1452 (C=C aromatic stretching) 1255 (C–OH stretching). ^{1}HNMR (DMSO, 300 MHz) δ: 11.00 (s, 1H, OH; 10.50 (s, 1H, OH); 8.75 (s, 1H, imine C-H); 7.42 (s, 1H, Ar-H, J = 8.6 Hz); 6.40 (dd, 1H, Ar-H, J = 2.4 Hz); 6.32(d, 1H, Ar-H, J = 2.1Hz); 2.4 (s, 2H, amine N-H); Mass (m/z): 151 (M-1)$^-$.

3.3.5. 4-((2-phenylhydrazono)methyl)benzene-1,3-diol (2)

IR (KBr cm^{-1}): 3504, 3423 (NH str); 3315 (OH-str); 3055, 3034 (Ar, C-H str); 1627 (C=N str); 1508, 1444 (C=C aromatic stretching) 1188, 1187 (C–OH stretching). ^{1}HNMR (DMSO, 300 MHz): 10.73 (s, 1H, OH); 10.11(s, 1H, OH); 9.66 (s, 1H, amine NH); 8.03 (s, 1H, imine CH); 7.27 (d, 1H, ArH, J = 8.1 Hz); 7.23 (t, 2H, Ar-H, J = 7.8 Hz); 6.89 (d, 2H, Ar-H, J = 7.8 Hz); 6.74 (t, 1H, Ar-H, J = 7.2 Hz); 6.32 (d, 1H, Ar-H, J = 2.2 Hz); 6.29 (s, 1H, s, Ar-H). Mass (m/z): 228(M+1)$^+$.

3.3.6. 4-((2-(2,4-dinitrophenyl)hydrazono)methyl)benzene-1,3-diol (3)

IR (KBr cm^{-1}): 3743, 3618 (NH str); 3556, 3269(OH str); 3099 (C-H, Ar str); 1614 (C=N str); 1510, 1330 (N-O str);1419 (C=C aromatic stretching); 1224, 1130 (C–OH stretching); 870 (C-N str of NO$_2$). ^{1}HNMR (DMSO, 300 MHz) δ: 11.40 (s, 1H, OH); 10.05 (s, 1H, OH); 9.66 (s, 1H, NH); 8.94 (s, 1H, imine CH); 8.57 (s, 1H, Ar-H); 8.24 (d, 1H, 1ArH, J = 8.3 Hz); 7.71 (d, 2H, 2Ar-H, J = 6.9 Hz); 6.33 (d, 2H, 2Ar-H, J = 6.1 Hz). Mass (m/z): 319 (M+1)$^+$.

3.3.7. 4-((benzylimino)methyl)benzene-1,3-diol (4)

IR (KBr cm^{-1}): 3741 (OH-str); 3024 (Ar, C-H str); 2873, 2291 (C-H str, methylene); 1643 (C=N str); 1535, 1454 (C=C aromatic stretching); 1242, 1203, 1170 (C–OH stretching). ^{1}HNMR (DMSO, 300 MHz) δ: 13.78 (s, 1H, OH); 9.96 (s, 1H, OH); 8.49(s, 1H, CH-imine); 7.27-7.38 (m, 5H, Ar-H); 7.23(d, 1H, Ar-H, J = 8.4 Hz); 6.30 (dd, 1H, Ar-H, J = 6.3 Hz); 6.17(d, 1H, Ar-H, J = 2.2 Hz); 4.70 (s, 2H, methylene). Mass (m/z): 226 (M-1)$^-$.

3.3.8. 4-((butylimino)methyl)benzene-1,3-diol (5)

IR (KBr cm^{-1}): 3732 (OH str); 3055 (C-H, Ar str); 2964 (C-H str, methyl); 2873 (C-H str, methylene); 1643 (C=N str); 1539, 1452 (C=C aromatic stretching) 1228, 1174, 1145 (C–OH stretching). ^{1}HNMR (DMSO, 300 MHz) δ: 13.90 (s, 1H, OH); 10.02 (s, 1H, OH); 8.30 (s, 1H, CH-imine);7.15 (d, 1H, Ar-H, J = 8.4 Hz); 6.23 (dd, 1H, Ar-H, J = 6.4 Hz); 6.12 (d, 1H, Ar-H, J = 2.9 Hz); 3.49 (t, 2H, CH$_2$, J = 6.7 Hz); 1.59 (pent, 2H, CH$_2$, J = 6.8 Hz); 1.35(hex, 2H, CH$_2$, J = 7.4 Hz); 0.91(t, 3H, CH$_3$, J = 7.3 Hz). Mass (m/z): 193 (M$^+$)$^+$.

3.3.9. 4-((phenylimino)methyl)benzene-1,3-diol (6)

IR (KBr cm^{-1}): 3722, 3311 (OH str); 3057 (C-H, Ar str); 1641 (C=N str); 1595, 1453 (C=C aromatic stretching) 1209, 1161, 1126 (C–OH stretching). ^{1}HNMR (DMSO, 300 MHz) δ: 13.54 (s, 1H, OH); 10.26 (s, 1H, OH); 8.78(s, 1H, CH-imine); 7.39-7.43 (m, 3H, Ar-H); 7.34 (d, 2H, Ar-H, J = 7.5 Hz); 7.26 (d, 1H, Ar-H, J = 7.2 Hz); 6.41 (dd, 1H, Ar-H, J = 6.3 Hz); 6.28 (d, 1H, Ar-H, J = 2.3 Hz). Mass (m/z): 213(M$^+$)$^+$.

3.3.10. 4-(((2-hydroxyphenyl)imino)methyl)benzene-1,3-diol (7)

IR (KBr cm^{-1}):3751, 3612, 3475(OH- stretching); 3051(aromatic C-H stretching); 1618 (C=N stretching); 1591, 1489 (C=C aromatic stretching); 1234, 1195, 1161, 1126 (C–OH stretching). ^{1}HNMR (DMSO, 300 MHz) δ: 14.24 (s, 1H, OH); 10.16 (s, 1H, OH);9.66 (s, 1H, OH); 8.76(s, 1H, imine C-H); 7.36-7.27(m, 2H, ArH) 7.08–7.02 (m, 1H, Ar-H); 6.92-6.81 (m, 2H, Ar-H); 6.34 (dd, 1H, Ar-H, J = 6.3 Hz); 6.22 (d, 1H, Ar-H, J = 2.1 Hz). Mass (m/z): 229 (M$^+$)$^+$.

3.3.11. 4-(((4-fluorophenyl)imino)methyl)benzene-1,3-diol (8)

IR (KBr cm^{-1}): 3745 (OH- stretching); 3026 (aromatic C-H stretching); 1645 (C=N str); 1512, (C=C aromatic stretching); 1240, 1163 (C–OH stretching); 1122(C-F str). ^{1}HNMR (DMSO, 300 MHz) δ: 13.34 (s, 1H, OH); 10.25 (s, 1H, OH); 8.76 (s, 1H, imine C-H); 7.53 (d,

7

1H, Ar-H, J = 8.6 Hz); 7.42-7.36 (m, 2H, Ar-H); 7.27–7.21 (m, 1H, Ar-H); 6.41(dd, 1H, Ar-H, J = 6.3 Hz); 6.22 (d, 1H, Ar-H, J = 2.1 Hz). Mass m/z): 232(M+1)$^+$.

3.3.12. 4-((naphthalen-1-ylimino)methyl)benzene-1,3-diol (9)

IR (KBr cm^{-1}): 3741 (OH stretching); 3051 (aromatic C-H stretching); 1616 (C=N stretching imine); 1541, 1514, 1481 (C=C aromatic stretching); 1220, 1185, 1157 (C–OH stretching); 839, 796, 769, 623 (C-H oop bending, polynuclear aromatic). ^{1}HNMR (DMSO, 300 MHz) δ: 13.59 (s, 1H, OH); 10.35 (s, 1H, OH); 8.85 (s, 1H, imine C-H); 8.13-7.80 (m, 3H, Ar-H); 7.56–7.37 (m, 5H, Ar-H); 6.45 (d, 2H, Ar-H, J = 6.5 Hz); 6.37 (s, 1H, Ar-H). Mass (m/z): 263(M$^+$)$^+$.

3.3.13 4-((2,4-dihydroxybenzylidene)amino)-3-hydroxynaphthalene-1-sulfonic acid (10)

IR (KBr cm^{-1}): 3745, 3608 (OH stretching); 3093 (aromatic C-H stretching); 1616 (C=N stretching imine); 1521, 1471, 1411 (C=C aromatic stretching); 1340, 1136 (S=O stretching); 1222, 1168, 1107, 1049 (C-OH stretching); 850 (S–O stretch). ^{1}HNMR (DMSO, 300 MHz) δ: 11.06 (s, 1H, OH); 10.75 (s, 1H, OH); 9.91 (s, 1H, OH); 8.93 (s, 1H, imine C-H); 8.80 (d, 2H, Ar-H, J= 8.7 Hz); 7.90 (s, 1H, Ar); 7.87-7.76 (m, 2H, Ar-H); 7.59–7.50 (m, 1H, Ar-H); 7.43 (t, 1H, Ar-H, J = 7.6 Hz); 6.56 (d, 1H, Ar-H, J = 1.8 Hz); 3.85 (s, 1H, SO$_3$H). Mass (m/z): 360 (M+1)$^+$.

3.3.14. 4-((thiazol-2-ylimino)methyl)benzene-1,3-diol (11)

IR (KBr cm^{-1}): 3745, 3682 (OH stretching); 3026 (aromatic C-H stretching); 1645 (C=N stretching imine); 1514 (C=C aromatic stretching); 1336, 1317 (thiazole skeletal bands); 1249, 1195, 1151 (C–OH stretching). ^{1}HNMR (DMSO, 300 MHz) δ: 12.00 (s, 1H, OH); 10.57 (s, 1H, OH); 9.08 (s, 1H, imine C-H); 7.64 (d, 1H, Ar-H, J = 7.9 Hz); 7.57 (d, 1H, Ar-H, J = 4.3 Hz); 6.91-6.87 (m, 1H, Ar-H); 6.44 (dd, 1H, Ar-H, J = 7.1 Hz); 6.36 (d, 1H, Ar-H, J = 5.7 Hz). Mass (m/z): 221(M+1)$^+$.

3.3.15. 4-((benzo[d]thiazol-2-ylimino)methyl)benzene-1,3-diol (12)

IR (KBr cm^{-1}): 3739 (OH stretching); 3047 (aromatic C-H stretching); 1629 (C=N stretching imine); 1598, 1504, 1446 (C=C aromatic stretching); 1344, 1311 (thiazole skeletal bands); 1242, 1188, 1116 (C–OH stretching). ^{1}HNMR (DMSO, 300 MHz) δ:11.95 (s, 1H, OH);10.73 (s, 1H, OH); 9.24 (s, 1H, CH imine); 8.03 (d, 1H, Ar-H, J= 7.8);7.89(d, 1H, Ar-H, J= 7.8 Hz); 7.75(d, 1H, Ar-H, J = 8.6 Hz); 7.50 (t, 1H, Ar-H, J = 7.2 Hz); 7.40 (t, 1H, Ar-H, J = 7.5 Hz); 6.40 (d, 1H, Ar-H, J = 8.1 Hz); 6.30 (s, 1H, Ar-H). Mass (m/z): 272(M+2)$^+$

3.3.16. 4-(((4-(1H-benzo[d]imidazol-2-yl)phenyl)imino)methyl)benzene-1,3-diol (13)

IR (KBr cm^{-1}): 3545 (N-H str, benzothiazole); 3107(OH stretching); 3064 (aromatic C-H stretching); 1629 (C=N stretching imine); 1539, 1504, 1448 (C=C aromatic stretching); 1396, 1359 (thiazole skeletal bands); 1284, 1255, 1211 (C–OH stretching). ^{1}HNMR (DMSO, 300 MHz): 13.45 (s, 1H, OH);12.91(s, 1H, OH); 10.35 (s, 1H, amine NH); 8.90 (s, 1H, imine CH); 8.23 (d, 2H, ArH, J = 8.4 Hz); 7.66 (d, 2H, Ar-H, J = 6.6 Hz); 7.54 (d, 2H, Ar-H, J = 8.7 Hz); 7.47 (d, 2H, Ar-H, J = 8.7 Hz); 7.20 (d, 1H, Ar-H, J = 4.8 Hz); 6.44 (dd, 1H, Ar-H, J = 6.3 Hz); 6.31 (d, 1H, Ar-H, J= 2.1 Hz). 328 (M-1)$^-$.

8

3.3. Malachite green assay for Hsp90 ATPase suppression

The malachite green enzyme inhibition assay for validating our docking methodology revealed that all the azomethines are potent Hsp90 inhibitors with an IC_{50} value of less than 3.1 µM (**Table 3**). Compound **9** and **11** showed maximum inhibitory potential with an IC_{50} value of 0.02 µM. The results summarized in **Table 3** further revealed that the software predicted potency of the compounds (docking score) did not match with their biological results. This mismatch can be explained from the H-bond interactions of the molecules at the N-terminal ATP binding site of Hsp90. The schiff base derived from 2,4-dinitro phenyl hydrazine (**3**) was the top scored ligand because of more hydrogen bond contact with the protein. However in some cases excess of hydrogen bond between ligand and protein resulted in reduced activity as few interactions are necessary for effective inhibition. An insight into the hydrogen bond interaction of the two most potent compounds (**9** and **11**) revealed some interesting facts regarding their binding affinity. Both of them were found to interact with different amino acids and water molecules in the catalytic site of Hsp90. Ligand **9** formed similar hydrogen bond contact like majority of the compounds in the series, i.e. 2'-OH with Asn51/water 903 and 4'-OH with Asp93/water 902 (**Fig. 7a**) . The 2' and 4' OH of **11** formed H-bond with Asp 54 whereas its imine nitrogen demonstrated hydrogen bond with water molecule 1026 (**Fig. 7b**).

3.4. *In vitro* cell growth assay

The IC_{50} values of the MTT assay against PC3 cells are given in **Table 3.** From the table it is evident that except **9** all the molecules in the series showed moderate to good cytotoxic effect. The most effective derivative was found to be **13,** which showed high cell kill in PC3 cell at IC_{50} of 4.85 µM. The schiff base **5** and **6** with an IC_{50} value of 7.43 µM and 7.15 µM respectively were the other promising anticancer molecules among the newly synthesized compounds. However unlike malachite green assay, none of the molecules demonstrated IC_{50} values in nanomolar range. The poor cell permeability of compound **3** and **10 (Table 4)** can be responsible for the aforementioned activity difference. For rest of the compounds this discrepancy can be attributed to rapid efflux of the molecules from the PC3 cells by MRP and GST proteins which are not clients of Hsp90[44-46]. However the proposed hypothesis needs to be substantiated practically by various biological experiments.

4. Conclusion

In summary, we have discovered novel 2,4-dihydroxy phenyl imines as potent and selective inhibitors of molecular chaperone Hsp90 with significant antiproliferative effect against PC3 carcinoma cells. The work was facilitated by a validated molecular docking methodology which identified additional amino acid and water molecule (Asp 54, water 903, 1026 for H-bond contact) crucial for effective protein suppression in addition to the reported ones(Asp 93, Asn 51, water 902 for H-bond contact). Our Hsp90 research effort did not establish any comprehensive structure-activity relationship for the synthesized imines. However, the rational drug design approach led to the discovery of high potency compounds with excellent ligand efficiency. Finally, compound **13** with sub micro-molar target affinity and good cellular potency was identified as an ideal molecule for pre-clinical evaluation in animals. Moreover this imine offers diverse synthetic routes for multiple chemical modifications. Furthermore, the simple and facile three step synthetic procedure for **13** will enable cost-effective scale up and optimization of this

molecule. Hence this schiff base can be regarded as a high quality viable lead structure for the future development of potent Hsp90 antagonists with fewer adverse effects.

Disclosure of interest

The authors declare that they have no conflicts of interest concerning this article.

Acknowledgement

References

[1] M.W. Hance, K.D. Nolan, J.S. Isaacs, Cancers. 6 (2014) 1065-1097.

[2] M. Taipale, D.F. Jarosz, S. Lindquist, Nat. Rev. Mol. Cell. Biol. 11 (2010) 515-528.

[3] K. Moulick, J.H. Ahn, H. Zong, A. Rodina, L. Cerchietti, E.M. Gomes DaGama, E. Caldas-Lopes, K. Beebe, F. Perna, K. Hatzi, L.P. Vu, X. Zhao, D. Zatorska, T. Taldone, P. Smith-Jones, M. Alpaugh, S.S. Gross, N. Pillarsetty, T. Ku, J.S. Lewis, S.M. Larson, R. Levine, H. Erdjument-Bromage, M.L. Guzman, S.D. Nimer, A. Melnick, L. Neckers, G. Chiosis, , Nat. Chem. Biol. 7 (2011) 818-826.

[4] P. Workman, Cancer. Lett. 206 (2004) 149-157.

[5] T. Didenko, A.M. Duarte, G.E. Karagoz, S.G. Rudiger, Biochim. Biophys. Acta. 1823 (2012) 636-647.

[6] C.K. Vaughan, P.W. Piper, L.H. Pearl, C. Prodromou, The FEBS J. 276 (2009) 199-209.

[7] C. Ban, W. Yang, Cell. 95 (1998) 541-552.

[8] S.M. Roe, C. Prodromou, R. O'Brien, J.E. Ladbury, P.W. Piper, L.H. Pearl, J. Med. Chem. 42 (1999) 260-266.

[9] A.M. Bilwes, C.M. Quezada, L.R. Croal, B.R. Crane, M.I. Simon, Nat. Struct. Biol. 8 (2001) 353-360.

[10] J.L. Johnson, Biochim. Biophys. Acta. 1823 (2012) 607-613.

[11] J.M. Eckl, K. Richter, Int. J. Biochem. Mol. Biol. 4 (2013) 157-165.

[12] S.D. Hartson, R.L. Matts, Biochim. Biophysic. Acta. 1823 (2012) 656-667.

[13] C.L. McDowell, R. Bryan Sutton, W.M. Obermann, Int. J. Biol. Macromol. 45 (2009) 310-314.

[14] E. Yuriev, P.A. Ramsland, J. Mol. Recogn. 26 (2013) 215-239.

[15] R. Garcia-Carbonero, A. Carnero, L. Paz-Ares, The Lancet. Oncol. 14 (2013) e358-369.

[16] A. Gopalsamy, M. Shi, J. Golas, E. Vogan, J. Jacob, M. Johnson, F. Lee, R. Nilakantan, R. Petersen, K. Svenson, R. Chopra, M.S. Tam, Y. Wen, J. Ellingboe, K. Arndt, F. Boschelli, J. Med. Chem. 51 (2008) 373-375.

[17] K. Sztanke, A. Maziarka, A. Osinka, M. Sztanke, Biorg. Med. Chem. 21 (2013) 3648-3666.

[18] A. Ganguly, P. Chakraborty, K. Banerjee, S.K. Choudhuri, Eur. J. Pharm. Sci. 51 (2014) 96-109.

[19] S. Dutta Gupta, D. Snigdha, G.I. Mazaira, M.D. Galigniana, C.V. Subrahmanyam, N.L. Gowrishankar, N.M. Raghavendra, Biomed. Pharmacother. 68 (2014) 369-376.

[20] S. Dutta Gupta, C.V.S. Subrahmanyam, N.M. Raghavendra, Biofes-2012, Leonia International Convention Centre, Hyderabad, India (12-13 December, 2012).

[21] P.P. Kung, L. Funk, J. Meng, M. Collins, J.Z. Zhou, M.C. Johnson, A. Ekker, J. Wang, P. Mehta, M.J. Yin, C. Rodgers, J.F. Davies, 2nd, E. Bayman, T. Smeal, K.A. Maegley, M.R. Gehring, Bioorg. Med. Chem. Lett. 18 (2008) 6273-6278.

[22] A.N. Jain, J. Comput. Aided. Mol. Des. 21 (2007) 281-306.

[23] P.P. Kung, P.J. Sinnema, P. Richardson, M.J. Hickey, K.S. Gajiwala, F. Wang, B. Huang, G. McClellan, J. Wang, K. Maegley, S. Bergqvist, P.P. Mehta, R. Kania, Bioorg. Med. Chem. Lett. 21 (2011) 3557-3562.

[24] A. Yan, G.H. Grant, W.G. Richards, J. R. Soc. Interface. 6 (2008).

[25] M. Rarey, B. Kramer, T. Lengauer, J. Comput. Aided. Mol. Des. 11 (1997) 369-384.

[26] R. Wang, Y. Lu, S. Wang, J. Med. Chem.46 (2003) 2287-2303.

[27] R. Wang, Y. Lu, X. Fang, S. Wang, J. Chem. Inf. Comp. Sci. 44 (2004) 2114-2125.

[28] T. Cheng, X. Li, Y. Li, Z. Liu, R. Wang, J. Chem. Inf. Model. 49 (2009) 1079-1093.

11

[29] Y. Li, L. Han, Z. Liu, R. Wang, Journal of chemical information and modeling, 54 (2014) 1717-1736.

[30] W.L. Mendelson, S. Hayden, Synth. Commun. 26 (1996) 603-610.

[31] R. Dubey, N.S. Hari Narayana Moorthy, Chem. Pharm. Bull. 55 (2007) 115-117.

[32] T. Scheibel, S. Neuhofen, T. Weikl, C. Mayr, J. Reinstein, P.D. Vogel, J. Buchner, J. Biol. Chem. 272 (1997) 18608-18613.

[33] M. Rowlands, C. McAndrew, C. Prodromou, L. Pearl, A. Kalusa, K. Jones, P. Workman, W. Aherne, J. Biomol. Screen. 15 (2010) 279-286.

[34] K.W. Harder, P. Owen, L.K. Wong, R. Aebersold, I. Clark-Lewis, F.R. Jirik, Biochem. J. 298 (1994) 395-401.

[35] C. Avila, B.A. Kornilayev, B.S. Blagg, Bioorg. Med. Chem. 14 (2006) 1134-1142.

[36] M.G. Rowlands, Y.M. Newbatt, C. Prodromou, L.H. Pearl, P. Workman, W. Aherne, Anal. Biochem. 327 (2004) 176-183.

[37] D.A. Scudiero, R.H. Shoemaker, K.D. Paull, A. Monks, S. Tierney, T.H. Nofziger, M.J. Currens, D. Seniff, M.R. Boyd, Cancer. Res. 48 (1988) 4827-4833.

[38] P.W. Sylvester, Methods. Mol. Biol. 716 (2011) 157-168.

[39] N.J. Marshall, C.J. Goodwin, S.J. Holt, Growth. Regul. 5 (1995) 69-84.

[40] B.S. Creaven, B. Duff, D.A. Egan, K. Kavanagh, G. Rosair, V.R. Thangella, M. Walsh, Inorganica Chim. Acta. 363 (2010) 4048-4058.

[41] M.S. Refat, I.M. El-Deen, H.K. Ibrahim, S. El-Ghool, Spectrochim. Acta. Mol. Biomol. Spectrosc. 65 (2006) 1208-1220.

[42] K.K. Upadhyay, A. Kumar, S. Upadhyay, P.C. Mishra, J. Mol. Struc. 873 (2008) 5-16.

[43] A.J. Abdulghani, A.M. Khaleel, Bioinorg. Chem. App. 2013 (2013) 1-14.

[44] X. Liu, Z. Yan, L. Huang, M. Guo, Z. Zhang, C. Guo, Oncol. Rep. 25 (2011) 1343-1351.

[45] J.P. van Brussel, G.J. van Steenbrugge, J.C. Romijn, F.H. Schroder, G.H. Mickisch, Eur. J. Cancer. 35 (1999) 664-671.

[46] G.L. David-Beabes, M.J. Overman, J.A. Petrofski, P.A. Campbell, A.M. de Marzo, W.G. Nelson, Int. J. Oncol. 17 (2000) 1077-1086.

Fig. 1. Previously reported potent Hsp90 inhibitors.

Fig. 2. Most promising molecule discovered.

Fig. 3. General structure of synthesized imines along with the numbering system used.

Fig. 4. General scheme of synthesis of Schiff bases derived from 2,4-dihydroxy benzaldehyde.

Fig. 5a. Software generated hydrogen bond contacts (white bold line) of the native ligand with Hsp90 protein.

**Fig. 5b.** Hydrophobic interaction (white speheres) between ligand and protein as per the docking programme.

Fig. 6a. Hydrogen bond contact(white bold line)of **3**(ball and stick model) with amino acid residue (ball and stick model) and water molecule (ball and stick model) of 3EKR protein.

Fig. 6b. Hydrophobic interaction of ligand **3**(ball and stick model) and Hsp90 protein (PDB ID: 3EKR). The spheres indicates hydrophobic amino acids.

Fig. 7a. Hydrogen bond contact(white bold line) of **9**(ball and stick model) with amino acid residue (ball and stick model) and water molecule (ball and stick model) of 3EKR protein.

Fig. 7b. Hydrogen bond contact(white bold line) of **11**(ball and stick model) with amino acid residue (ball and stick model) and water molecule (ball and stick model) of 3EKR protein.

13

Fig. 1

A

B

Fig.2
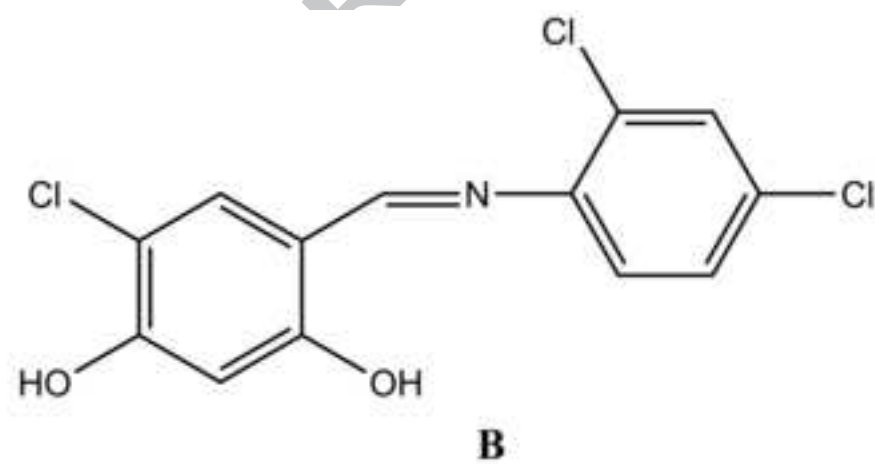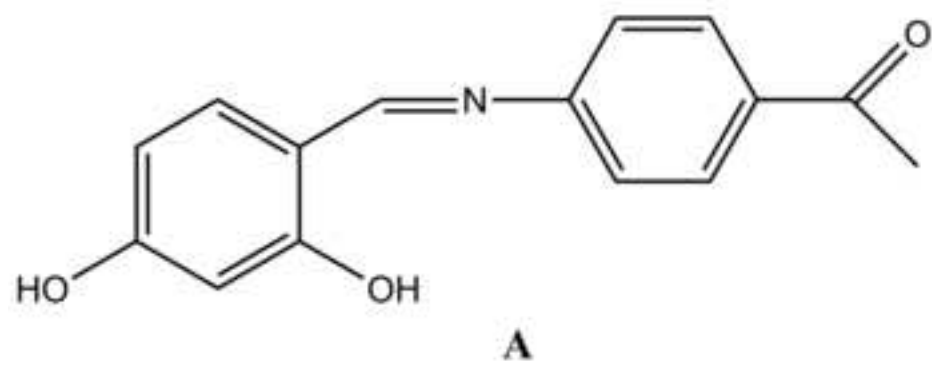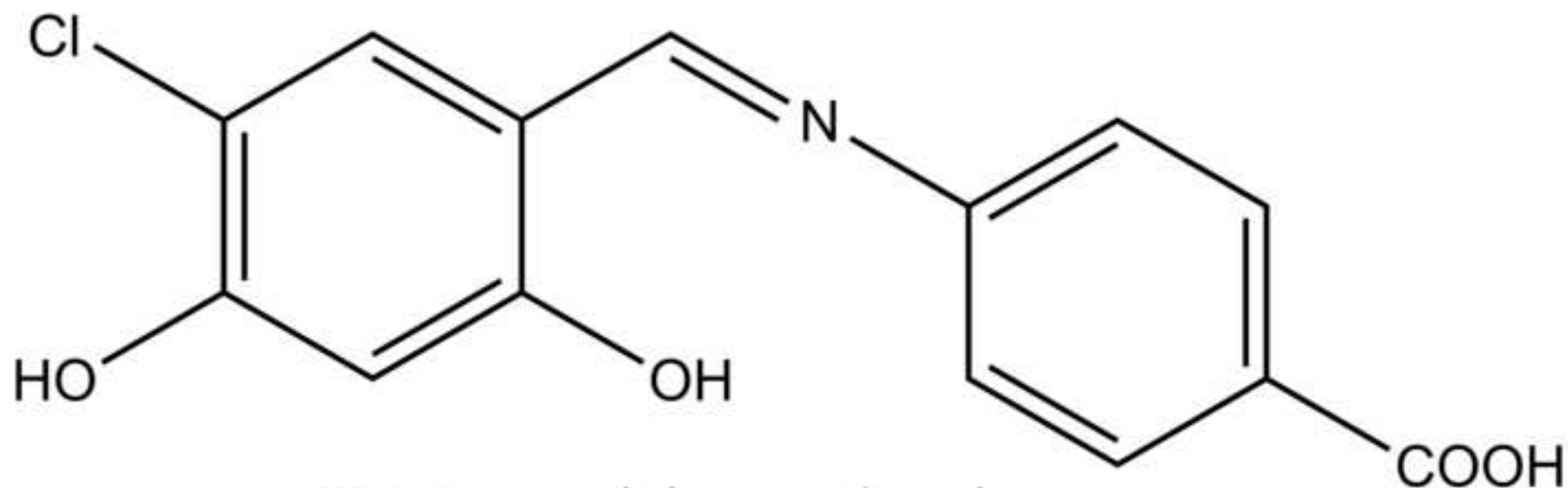
Most promising molecule

$IC_{50} = 0.52$ in enzyme inhibition assay.

$IC_{50} = 7.99$ in cell proliferation studies.

Fig.3

Fig.4

Compound 1: R= — NH₂   Compound 2: R=   Compound 3: R=   Compound 4: R=

Compound 5: R=   Compound 6: R=   Compound 7: R=   Compound 8: R=

Compound 9: R=   Compound 10: R=   Compound 11: R=   Compound 12: R=

Compound 13: R=

Fig.5a

Fig.5b

Fig.6a

Fig.6b
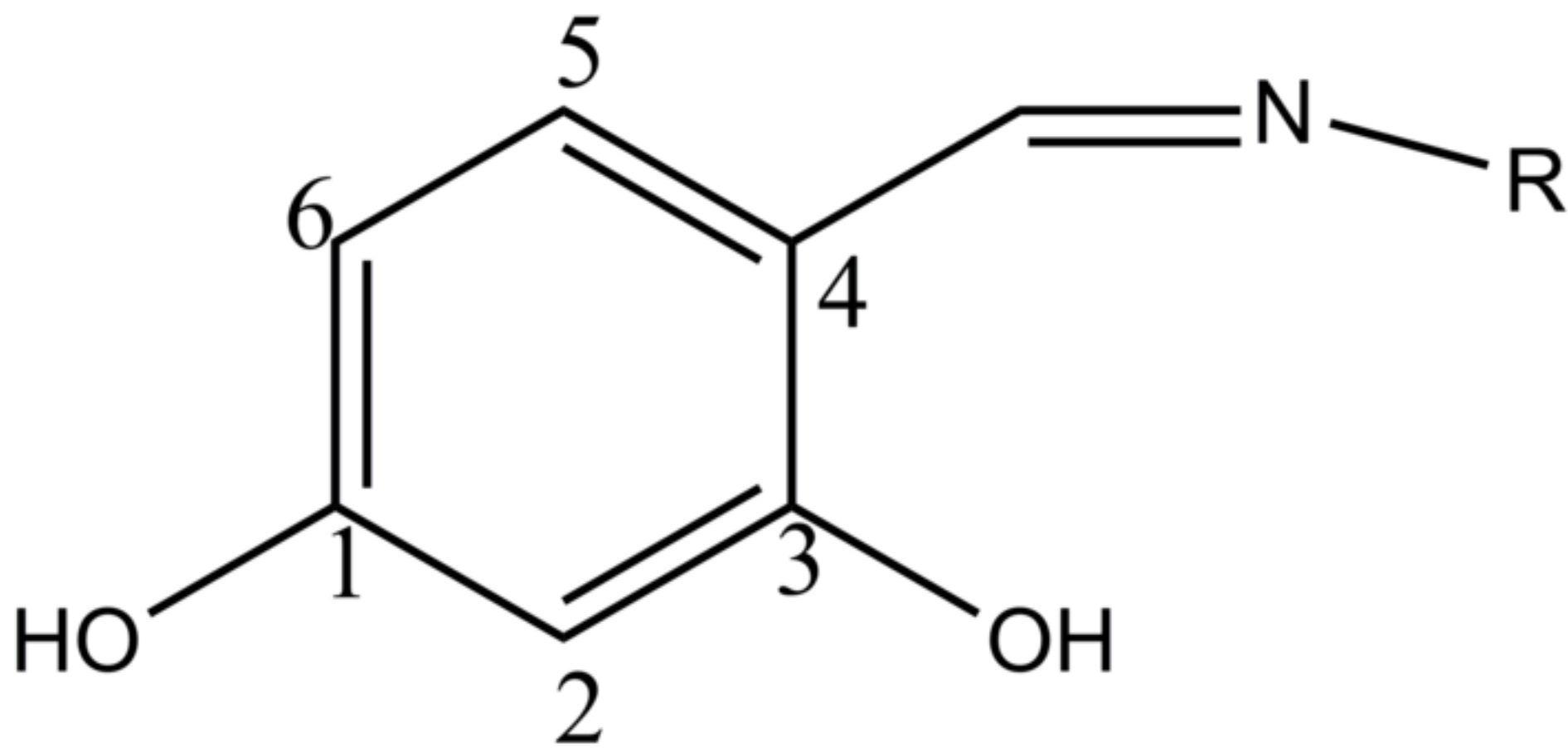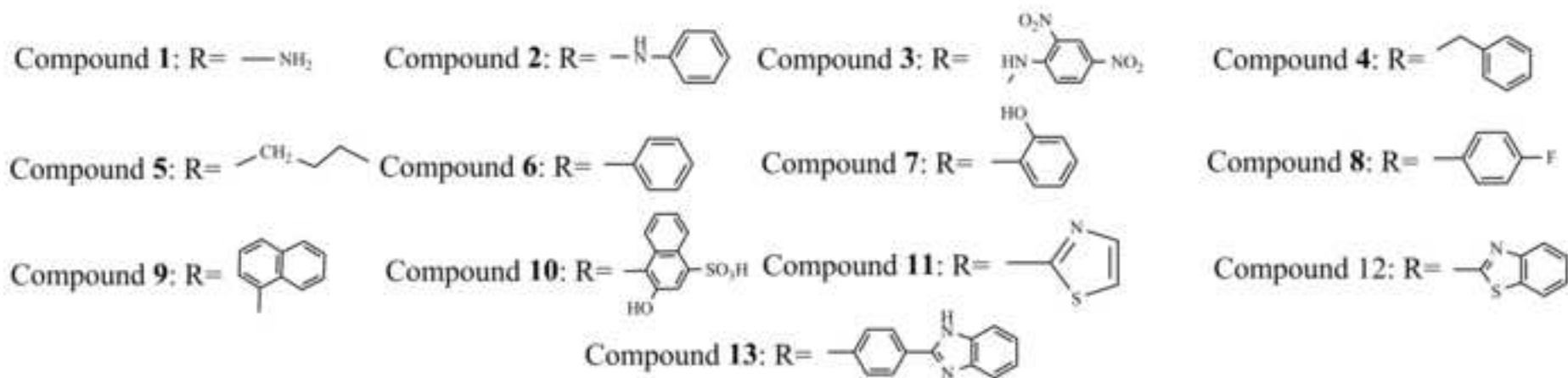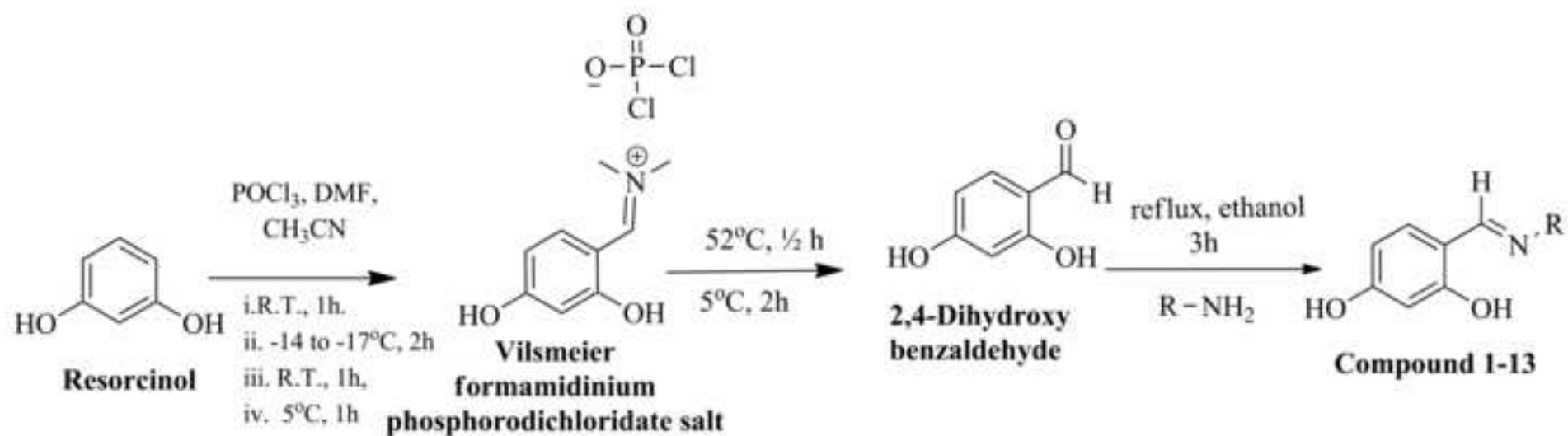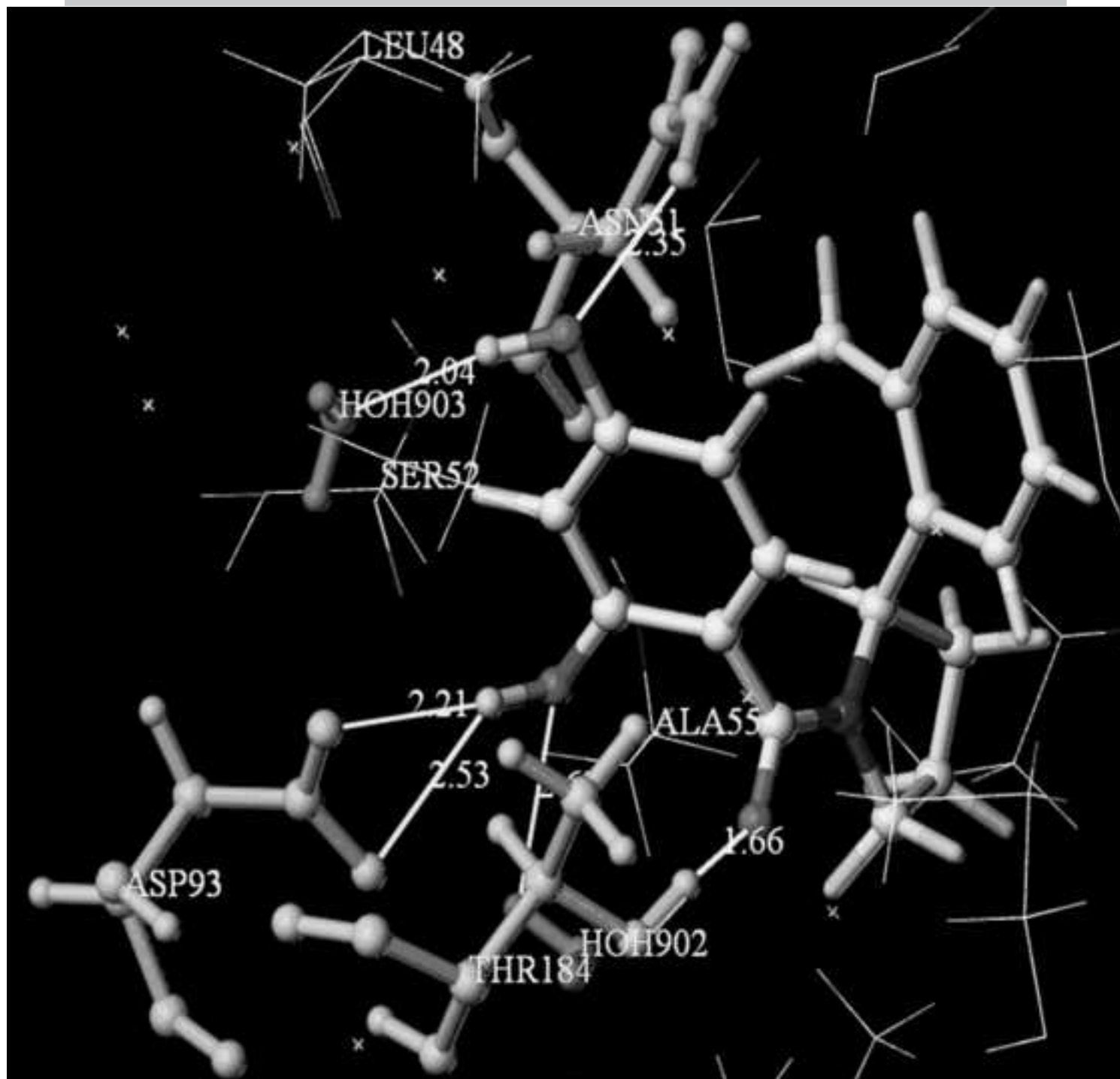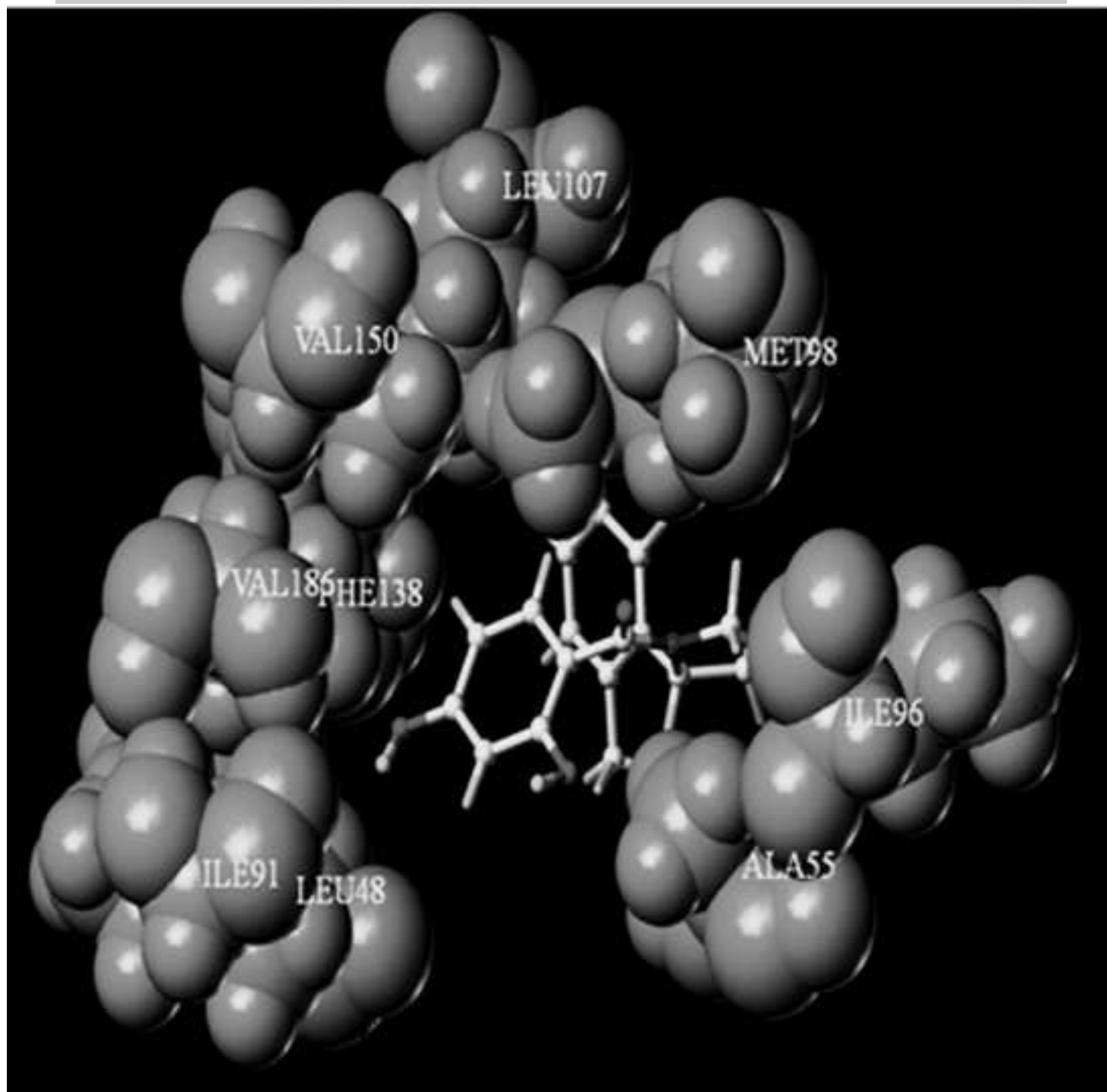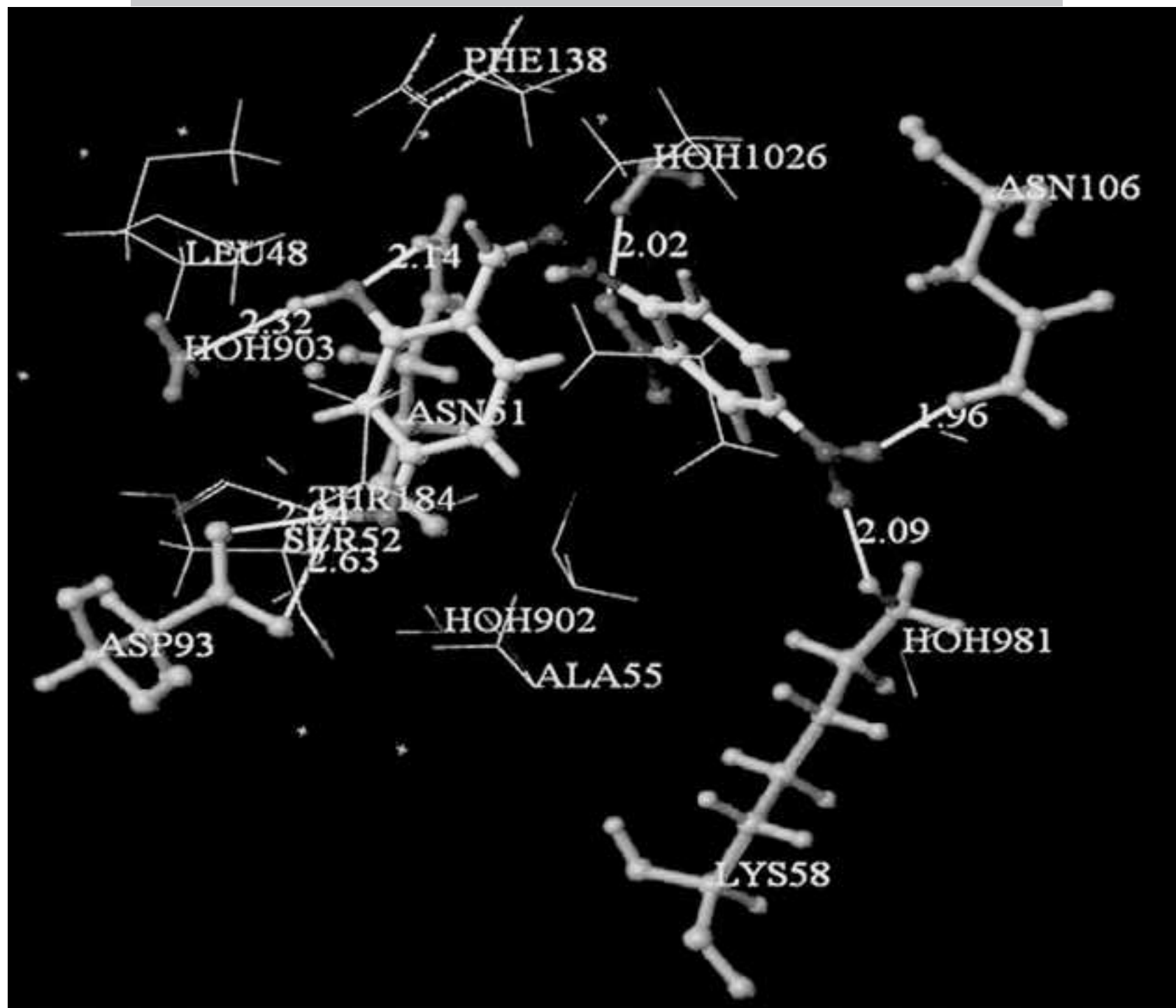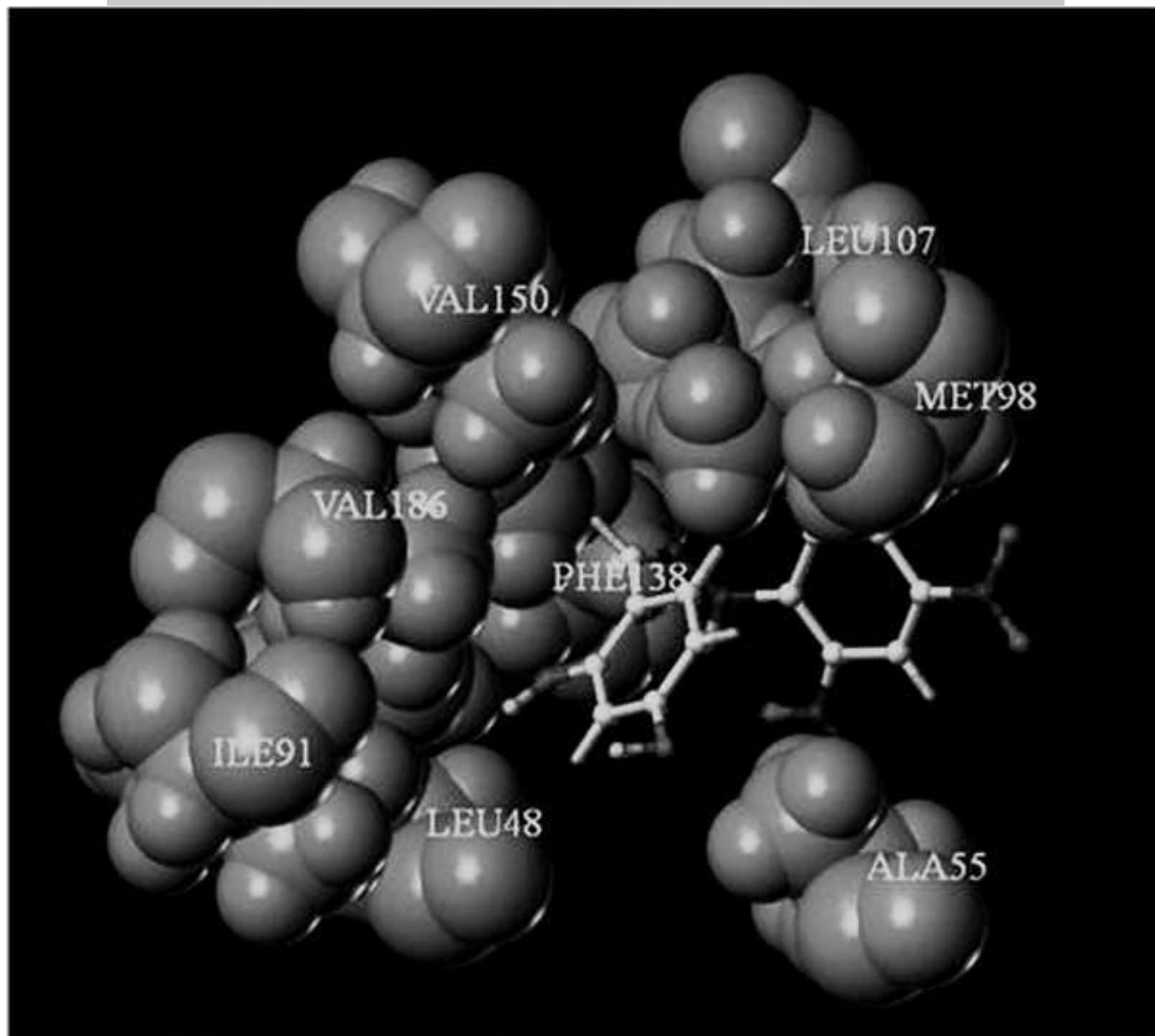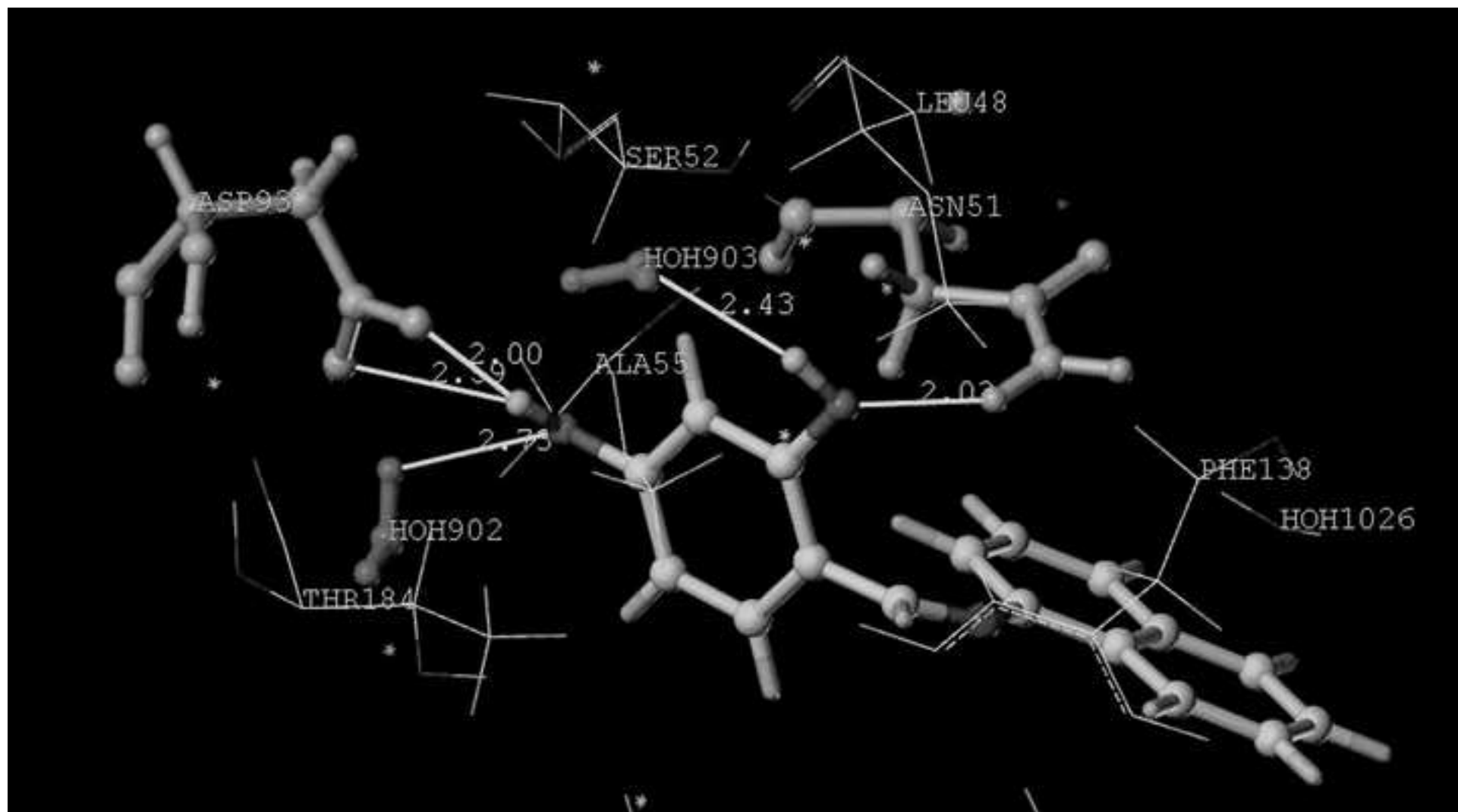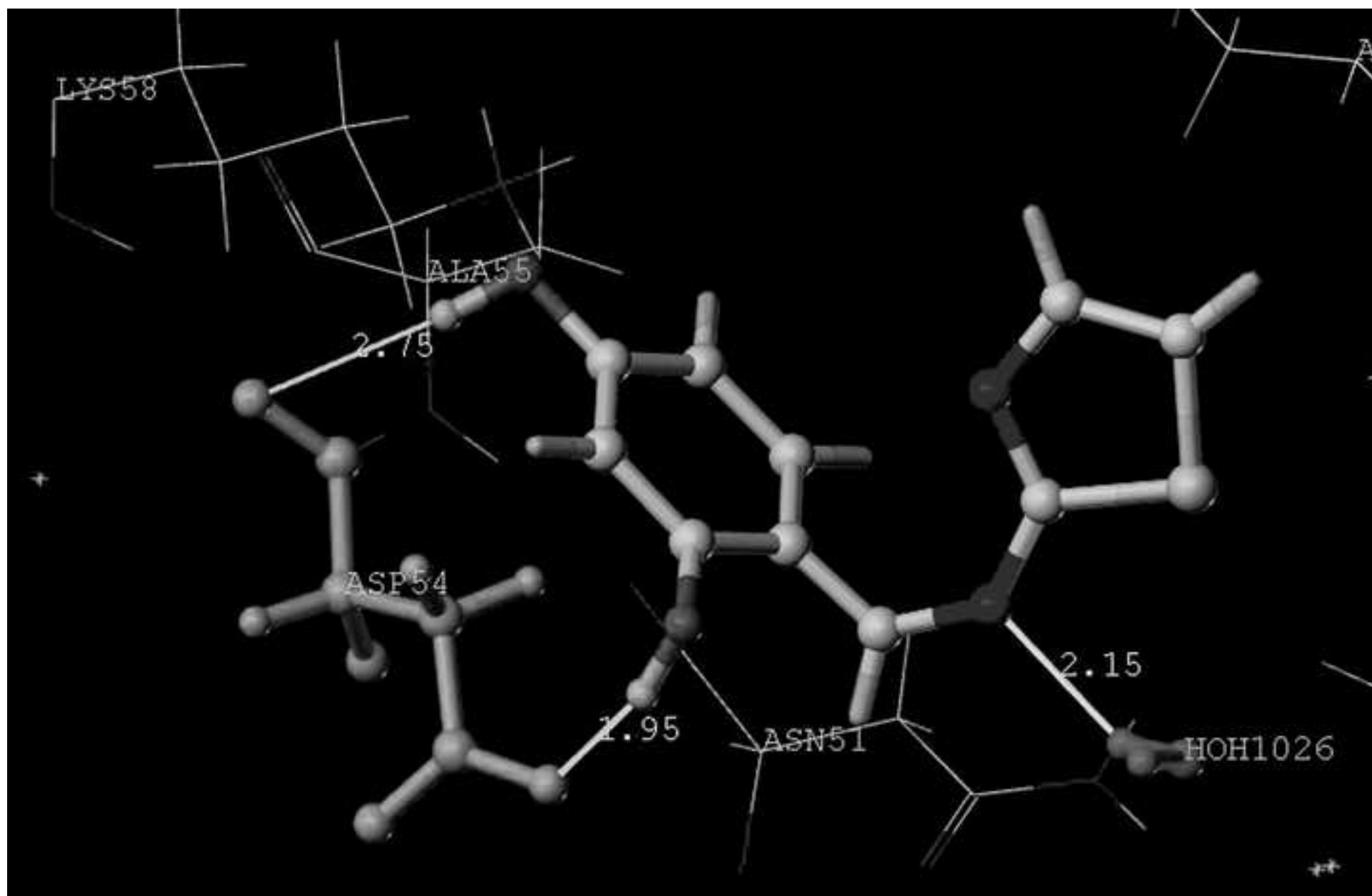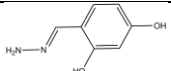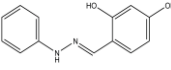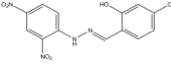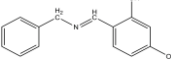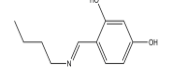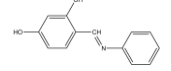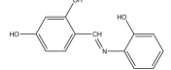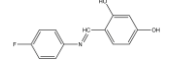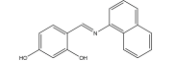
Table 1

Structure and molecular modelling results of the synthesized imines.

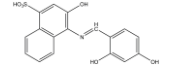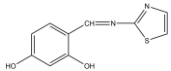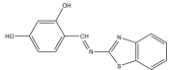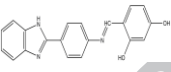| Compound	Structure	Total score	Crash	Polar	G score	PMF score	D score	Chem score	C score
1		4.27	-0.69	3.93	-100.40	-10.40	-59.37	-11.06	0
2		5.67	-0.70	2.78	-153.03	-7.04	-86.80	-15.13	1
3		7.65	-0.809	5.91	-128.89	-32.31	-108.92	-16.98	2
4		4. 36	-0.61	2.14	-108.24	-3.75	-77.06	-15.06	0
5		6.507	-1.22	2.15	-149.45	-3.57	-96.18	-13.66	2
6		5.04	-0.90	2.42	-117.68	-12.32	-88.92	-17.57	0
7		4.38	-1.06	0.97	-155.92	-8.09	-97.89	-15.86	2
8		4.97	-0.86	2.38	-118.59	-14.32	-90.51	-17.88	0
9		5.09	-0.79	2.45	-128.56	-13.74	-97.39	-20.13	2
10		5.91	-1.49	2.68	-163.08	-22.80	-125.43	-14.59	3
11		3.81	-0.90	2.31	-123.91	0.10	-71.04	-12.60	0
12		4.92	-0.67	2.37	-143.08	-16.49	-98.40	-1570	3
13		5.18	-0.74	3.40	-125.07	-20.26	-100.01	-20.82	3

Note:

C score: The consensus score: the sum of the number of 'good' results for each ligand in each scoring function. **G score:** It is based on hydrogen bonding, complex (ligand-protein), and internal (ligand-ligand). **PMF score**: It is the free energies of interactions for protein-ligand atom pairs. **D Score:** It is based on van der Waals interaction between protein and the ligand. **Chem score:** It includes terms for hydrogen bonding, metal-ligand interaction, lipophilic contact and rotational entropy, along with an intercept term. **Total score**: Total output of all the scores. **Crash:** The ability of the compound to penetrate the active site of the protein. **Polar: T**he polar interaction between the ligand and the protein

Table 2
Percent yield and physical parameters of the synthesized compounds[a].

Compound	Molecular weight	Melting point	R_f^a	%	Color/Physical state
1	152	248-250	0.35	69	yellow crystals
2	228	164-166	0.60	45	Light yellow crystals
3	318	202-203	0.75	51	Maroon crystals
4	227	168-170	0.67	80	yellow crystals
5	193	145-147	0.55	67	Orange crystals
6	213	168-170	0.70	65	Yellow crystals
7	229	146-147	0.56	79	Light orange crystals
8	231	101-103	0.67	90	yellow crystals
9	263	156-158	0.80	65	Orange crystals
10	359	230-233	0.67	78	Brown crystals
11	220	188-190	0.57	32	Yellow crystals
12	270	204-206	0.64	57	Orange crystals
13	329	245-248	0.68	45	Light brown crystals

[a]Determined in 50% ethylacetate/petroleum ether solvent system.

Table 3

Binding and growth inhibition assay results for compounds **1**-**13***.

Compound	Malachite green assay $IC_{50}(\mu M)$	MTT assay $IC_{50}(\mu M)$
1	0.29	13.37
2	0.06	19.12
3	2.50	22.65
4	0.04	56.16
5	0.03	7.43
6	3.09	7.15
7	0.94	30.03
8	0.13	13.38
9	0.02	>200
10	0.09	11.47
11	0.02	20.17
12	0.08	22.40
13	0.15	4.83
Geldanamycin	0.13	2.45

MTT: 3-(4,5-dimethylthiazol-2-yl)-2,5-diphenyl tetrazolium bromide

*Mean of three independent determinations

Table 4

Predicted cell membrane permeability and partition coefficient of the synthesized molecules*****

| Compound	Caco cell permeability	MDCK cell permeability	Log $P_{o/w}$
1	1354.92	1608.17	0.71
2	693.34	332.99	1.81
3	18.17	6.50	0.64
4	1183.02	593.26	2.70
5	1022.79	506.91	1.99
6	936.73	460.97	2.69
7	343.97	156.09	1.68
8	1080.35	973.36	3.01
9	1226.60	616.93	3.36
10	5.94	2.53	1.28
11	689.78	508.76	1.36
12	510.76	391.83	2.40
13	453.91	210.66	3.49

* Schrodinger software's QuickProp programme was employed for these calculations

Caco cell: cell line derived from human colorectal carcinoma.

MDCK cell: Madian-Darby canine kideney epithelial cells.

$P_{o/w}$ = partition coefficient calculated for n-octanol/water system.

Graphical abstract
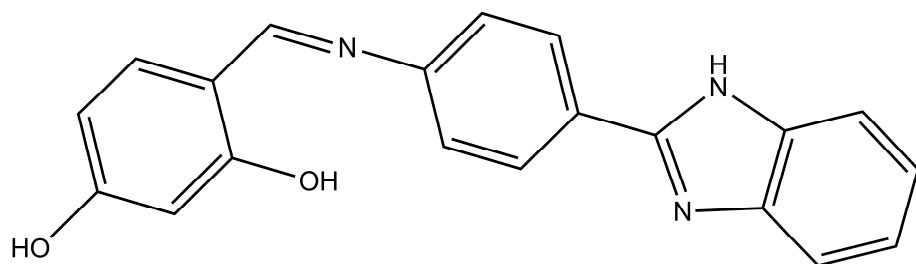
IC$_{50}$ value for Hsp90 inhibition = 0.15μM
IC$_{50}$ value in cell viability assay = 4.83μM

Highlights

- Structure based drug design of resorcyladehyde schiff bases as novel Hsp90 inhibitors.
- Potent molecules with IC_{50} value up to 0.02 µM in the protein inhibition assay.
- Significant antiproliferative effect of the compounds with IC_{50} value up to 4.83 µM.
- Generation of a lead molecule.